

Static Deflection Analysis of High Speed Integral Motor Spindle

Umesh B S¹, Shankara Murthy A G², Sanjay G.R³

¹Asst. Professor, Department of Mechanical Engg, Bapuji Institute of Engineering & Technology

² Professor, Department of Mechanical Engg, Bapuji Institute of Engineering & Technology

³ Senior Technical Lead, Damler Truck Innovation Center, Bengaluru

Abstract—The BT-40 Integral motor type milling spindle integrates a motor for enhanced performance and eliminates external power transmission constraints. This study optimizes spindle design through theoretical and FEA analysis of different bearing configurations. SOLIDWORKS models and ANSYS simulations assess deflection, stiffness, and natural frequencies. Bearing arrangement-1 with medium preload NSK bearings shows superior stiffness and operational stability, crucial for high-speed machining. This research emphasizes bearing selection's impact on spindle performance, guiding advancements in motorized spindle design for precision and longevity in industrial applications.

Index Terms— Bearing arrangement, Dynamic model, Static Deflection, Stiffness.

I. INTRODUCTION

Motorized spindles integrate a motor directly into the spindle shaft, eliminating the necessity of providing external power transmission such as belts or gears. This design enables the spindle to operate independently at higher speeds and with enhanced power efficiency. The integrated motor allows precise control of rotational speeds and accelerations, reducing vibrations and improving machining accuracy. High-precision bearings support the spindle shaft, ensuring smooth operation at maximum speeds while leveraging the motor's power characteristics.

The machine spindle's primary function is to drive either the work piece or the tool, depending on the machine type. Spindle accuracy relies on the elastic deformations of the spindle, its bearings, housing, and associated components. Overall stiffness significantly influences machining precision, influenced by bearing characteristics, preload settings, and operational forces.

Static deflection analysis assesses structural responses under steady loading conditions, excluding inertia and

damping effects. It calculates displacements, stresses, strains, and forces from loads without significant inertial or damping forces. This analysis provides an important insight about spindle performance and structural integrity under typical loads, aiding design optimization for reliable machining processes.

II. STATIC DEFLECTION ANALYSIS

Static deflection analysis evaluates steady loading effects on structures, focusing on displacements, stresses, strains, and forces without considering inertia and damping effects from time-varying loads. In engineering, machine failures due to spindle fatigue fractures are rare, but failures often result from self-excited vibrations caused by cutting forces, leading to significant spindle deformations. Therefore, the static design of milling spindles emphasizes spindle stiffness, crucial for load capacity and vibration resistance, key performance indicators for motorized spindles.

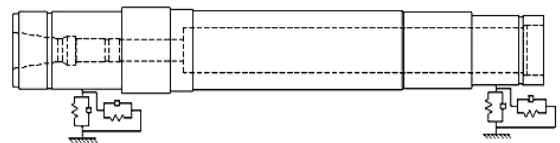


Fig. 2.1 Equivalent Dynamic model of the spindle

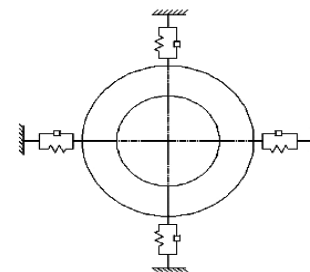


Fig. 2.2 Layout of spring damper unit

The spindle shaft is modeled using the BEAM188 element. It is a linear or quadratic beam element in 3-D. Each node, of this beam element has six degrees of freedom depending on the setting of KEYOPT(1). By default (KEYOPT(1)=0), each node has, translations and rotations along x, y, and z axes

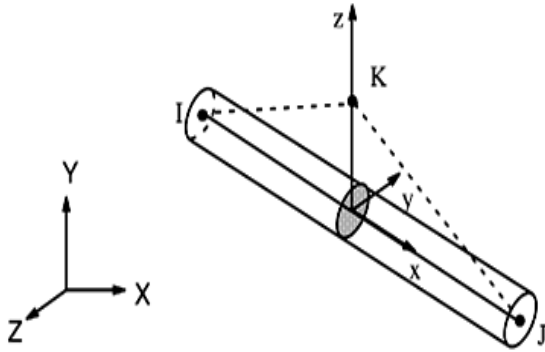


Fig. 2.3 BEAM 188 element geometry

A. BEAM188 Input Summary

Nodes- I, J, K (K being orientation node, is optional but recommended)
 Degrees of Freedom– UX, UY, UZ, ROTX, ROTY, ROTZ
 Material Properties- EX, (PRXY or NUXY), ALPX, DENS, GXY, GYZ, GXZ, DAMP
 The bearing set is modelled using the COMBIN14 spring element, which serves as a spring-damper unit. COMBIN14 is widely employed and offers longitudinal or torsional capabilities in 1-D, 2-D, or 3-D applications.
 For longitudinal spring-damper configurations, it functions as a tension-compression element with up to three degrees of freedom at each node, allowing translations in the nodal x, y, and z directions. It does not consider bending or torsion.
 In torsional spring-damper setups, COMBIN14 operates as a rotational element having three degrees of freedom at each node, facilitating rotations about the nodal x, y, and z axes without consideration of bending or axial loads.
 This element is defined by two nodes, a spring constant kkk, and damping coefficients cv1cv1cv1 and cv2cv2cv2. In static or undamped modal analyses, the damping capability remains unused.

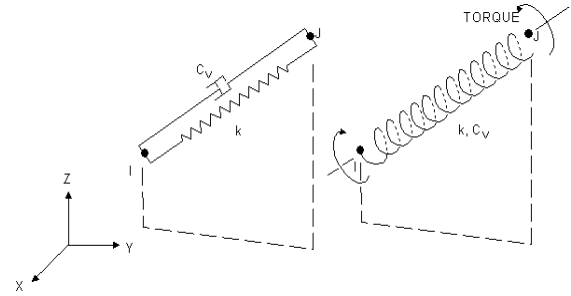


Fig. 2.4 COMBIN14 element geometry

B. COMBIN14 Input summary:

Node: I, J
 Degrees of freedom: UX, UY, UZ=0 and ROTX, ROTY, ROTZ=1
 Real constants: K-Spring constant

III. PERFORMING STATIC ANALYSIS

A. Elements type:

The elements chosen for the present work are BEAM188 and COMBIN14.

B. Real constants:

The real constants for COMBIN14 element i.e., Stiffness of spring ‘K’ for the representation of angular contact ball bearing sets are listed in TABLE 3.1

TABLE 3.1 Real constant for COMBIN14 element

Bearing location	Front bearings	Rear bearings
Real constant set number	1	2
Spring constant K, N/mm	624000	540000

TABLE 3.2 Beam sections considered for modeling of shaft

Beam section	1	2	3	4	5	6	7	8
Outer radius (mm)	32.5	32.5	32.5	32.5	36	34.5	29	27.5
Inner radius (mm)	22.2	18	16	14	14	14	14	18.1

C. Material properties: Modulus of elasticity of steel = 2.1×10^5 N/mm², Poisson’s ratio =0.3,Density = 7.82×10^{-6} Kg/mm³

D. Beam sections:

For modeling the spindle shaft, hollow circular beam sections having different values of inner and outer radius are considered. The beam sections considered for modelling of shaft are listed in TABLE 3.2.

E. Model generation:

The shaft bearing model in ANSYS is shown in Fig. 3.1.

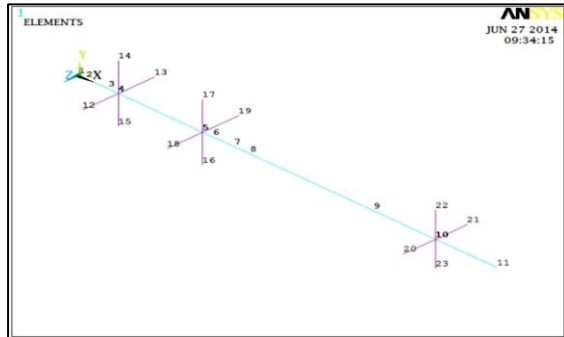


Fig 3.1 Shaft bearing model in ANSYS

F. Boundary conditions: A radial cutting force of 1217N, determined from theoretical calculations, is applied at the spindle nose end (Fig. 3.2). The nodes at both bearing sets are fully constrained to prevent any degrees of freedom

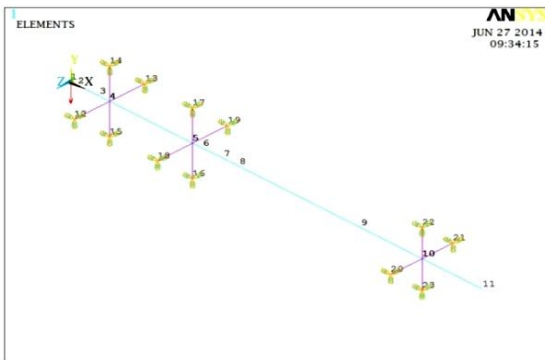


Fig 3.2 Boundary condition

IV. STATIC ANALYSIS OF BEARING ARRANGEMENTS

A. ANSYS static analysis results for bearing arrangement 1

The deflection at the spindle nose for different bearings under three preloading conditions is computed. Figures 4.1 to 4.3 show the results obtained for bearing arrangement 1 with NSK bearings

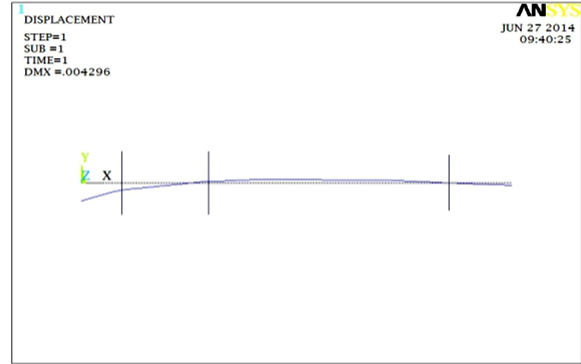


Fig. 4.1 Deflection at the spindle nose for NSK bearings (light preload)

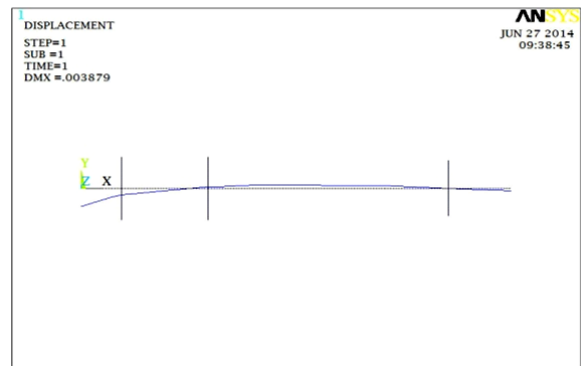


Fig. 4.2 Deflection at the spindle nose for NSK bearings (medium preload)

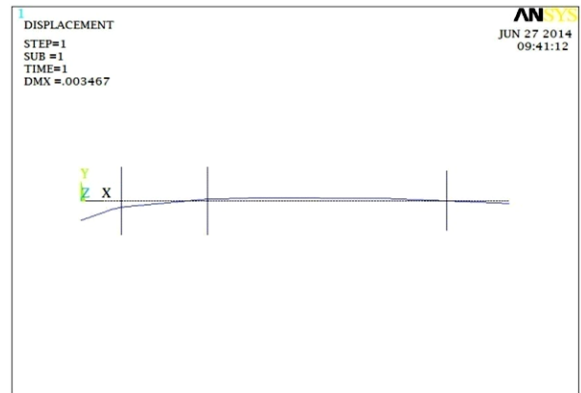


Fig. 4.3 Deflection at the spindle nose for NSK bearings (heavy preload)

B. ANSYS static analysis results for bearing arrangement 2

Fig.4.4 to Fig.4.6 show the results obtained for bearing arrangement 2 for NSK bearings.

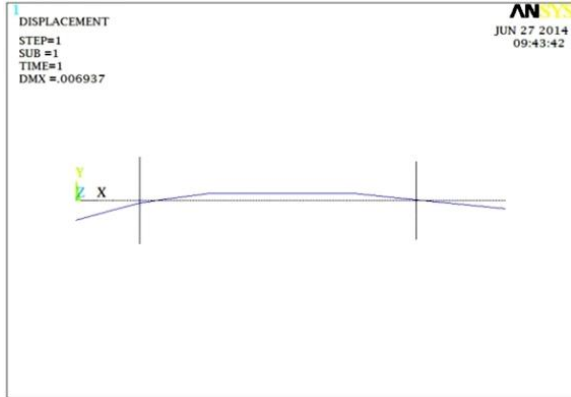


Fig. 4.4 Deflection at the spindle nose for NSK bearings (light preload)

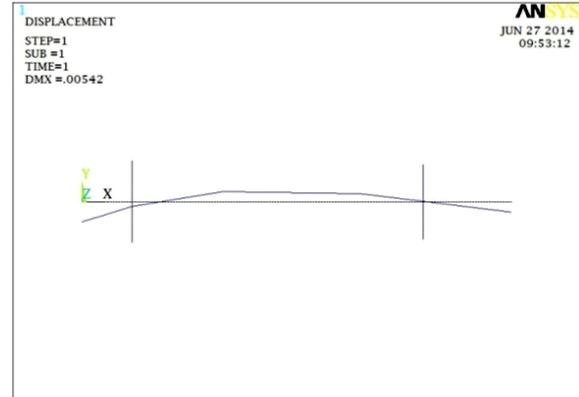


Fig. 4.7 Deflection at the spindle nose for NSK bearings (light preload)

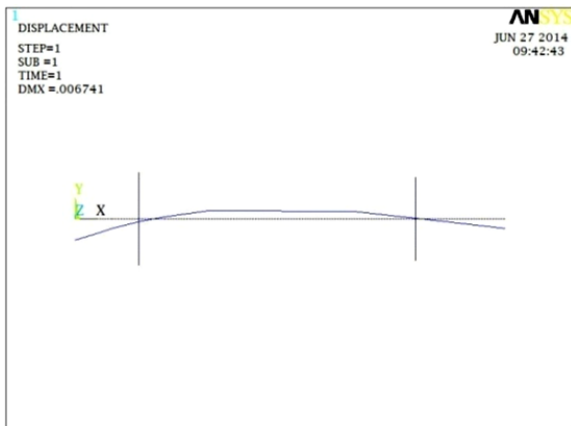


Fig 4.5 Deflection at the spindle nose for NSK bearings (medium preload)

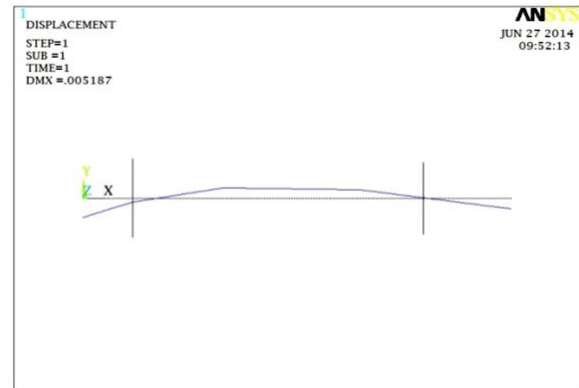


Fig. 4.8 Deflection at the spindle nose for NSK bearings (medium preload)

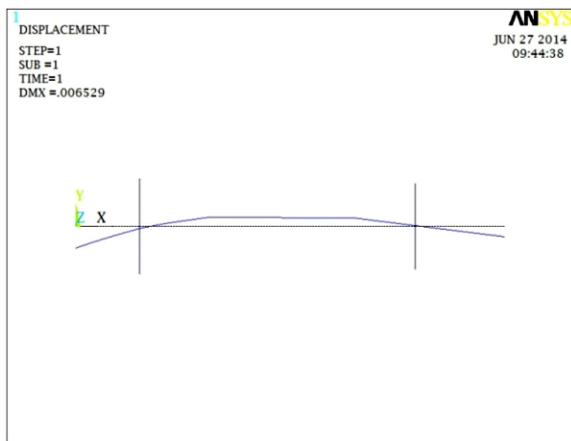


Fig 4.6 Deflection at the spindle nose for NSK bearings (heavy preload)



Fig. 4.9 Deflection at the spindle nose for NSK bearings (heavy preload)

C. ANSYS static analysis results for bearing arrangement 3

The results obtained for bearing arrangement 3 for NSK bearings are shown in Fig. 4.7 to Fig. 4.9.

Static deflection analysis for various bearings was conducted using ANSYS under light, medium, and heavy preloading conditions. Tables 4.1 to 4.10 shows the results compared with theoretical calculations.

TABLE 4.1 Bearing Arrangement 1: Light Preload

Bearings	Theoretical		ANSYS	
	Deflection (μm)	Stiffness ($\text{N}/\mu\text{m}$)	Deflection (μm)	Stiffness ($\text{N}/\mu\text{m}$)
NSK	4.37	278.4897	4.29	283.683
Timken	5.93	205.2277	6.04	201.4901
FAG	6.20	196.2903	6.47	188.0989
SKF	4.97	244.8692	5.08	239.5669

TABLE 4.2 Bearing Arrangement 1: Medium Preload

Bearings	Theoretical		ANSYS	
	Deflection (μm)	Stiffness ($\text{N}/\mu\text{m}$)	Deflection (μm)	Stiffness ($\text{N}/\mu\text{m}$)
NSK	4.01	303.4913	3.87	314.4703
Timken	4.80	253.5417	4.72	257.839
FAG	5.07	240.0394	5.04	241.4683
SKF	4.34	280.4147	4.25	286.3529

TABLE 4.3 Bearing Arrangement 1: Heavy Preload

Bearings	Theoretical		ANSYS	
	Deflection (μm)	Stiffness ($\text{N}/\mu\text{m}$)	Deflection (μm)	Stiffness ($\text{N}/\mu\text{m}$)
NSK	3.74	325.4011	3.46	351.7341
Timken	4.31	282.3666	4.16	292.5481
FAG	4.36	279.1284	4.30	283.0233
SKF	3.84	316.9271	3.57	340.8964

TABLE 4.4 Bearing Arrangement 2: Light Preload

Bearings	Theoretical		ANSYS	
	Deflection (μm)	Stiffness ($\text{N}/\mu\text{m}$)	Deflection (μm)	Stiffness ($\text{N}/\mu\text{m}$)
NSK	7.52	161.8351	6.93	174.3553
Timken	9.24	131.71	7.86	154.8346
FAG	10.3	118.1553	8.39	145.0536
SKF	8.02	151.7456	7.24	168.0939

TABLE 4.5 Bearing Arrangement 2: Medium Preload

Bearings	Theoretical		ANSYS	
	Deflection (μm)	Stiffness ($\text{N}/\mu\text{m}$)	Deflection (μm)	Stiffness ($\text{N}/\mu\text{m}$)
NSK	7.21	168.7933	6.74	179.4985
Timken	7.98	152.5063	7.12	170.927
FAG	8.39	145.0536	7.38	164.9051
SKF	7.20	169.0278	6.78	179.4985

TABLE 4.6 Bearing Arrangement 2: Heavy Preload

Bearings	Theoretical		ANSYS	
	Deflection (μm)	Stiffness ($\text{N}/\mu\text{m}$)	Deflection (μm)	Stiffness ($\text{N}/\mu\text{m}$)
NSK	6.82	178.4457	6.52	185.2359
Timken	7.39	164.682	6.84	177.924
FAG	7.64	159.2932	7.01	173.6091
SKF	7.05	172.6241	6.75	180.2963

TABLE 4.8 Bearing Arrangement 3: Light Preload

Bearings	Theoretical		ANSYS	
	Deflection (μm)	Stiffness ($\text{N}/\mu\text{m}$)	Deflection (μm)	Stiffness ($\text{N}/\mu\text{m}$)
NSK	6.57	185.2359	5.42	224.5387
Timken	8.61	141.3473	6.13	198.5318
FAG	9.85	123.5533	6.93	175.6133
SKF	7.11	171.1674	5.75	211.6522

TABLE 4.9 Bearing Arrangement 3: Medium Preload

Bearings	Theoretical		ANSYS	
	Deflection (μm)	Stiffness ($\text{N}/\mu\text{m}$)	Deflection (μm)	Stiffness ($\text{N}/\mu\text{m}$)
NSK	6.12	198.8562	5.18	234.9421
Timken	7.10	171.4085	5.41	224.9538
FAG	7.61	159.9212	5.77	210.9185
SKF	6.12	198.8562	5.18	234.9421

TABLE 4.10 Bearing Arrangement 3: Heavy Preload

Bearings	Theoretical		ANSYS	
	Deflection (μm)	Stiffness ($\text{N}/\mu\text{m}$)	Deflection (μm)	Stiffness ($\text{N}/\mu\text{m}$)
NSK	5.62	216.548	4.93	246.856
Timken	6.37	191.0518	5.06	240.5138
FAG	6.62	183.8369	5.24	232.2519
SKF	5.37	226.6294	4.57	266.302

The deflection at the spindle nose depends on bearing stiffness, span length, and overhang, affecting machining accuracy. Tables 4.1 to 4.10 compare theoretical and ANSYS-calculated deflections and stiffness. Bearing arrangement 1, with two front bearings in a quadruplet back-to-back setup, shows lower deflections, enabling higher speeds and resistance to tilting moments. At the rear, a single set of back-to-back bearings provides radial support. Medium preload conditions are suitable for spindle performance having optimal speed, rigidity, and reduced friction.

V. CONCLUSION

Static stiffness of the spindle assembly was analysed using ANSYS, employing BEAM188 and COMBIN14 elements to calculate spindle deflection. The results depicted a strong correlation in between theoretical calculations and ANSYS simulations. Notably, bearing arrangement 1, utilizing NSK bearings, exhibited lower deflection compared to other arrangements. This outcome underscores the

significant impact of overhang and bearing stiffness on spindle performance.

Optimizing spindle stiffness involves positioning bearings with higher stiffness at the front to minimize deflection. For this reason, bearing arrangement 1, featuring medium preloaded NSK bearings, is identified as the optimized configuration. This setup ensures enhanced speed, rigidity, and minimal temperature rise during operation, thereby optimizing spindle performance.

ACKNOWLEDGEMENT

The Authors sincerely acknowledge, All India Council for Technical Education (AICTE). New Delhi for funding this research Project under RPS Scheme

REFERENCES

- [1] Deping Liu and Hang Zhang, “Finite Element Analysis of High-Speed Motorized Spindle Based on ANSYS”, Journals of theoretical and applied mechanics, 2011.
- [2] Tony L. Schmitz, Nagaraj Arakere, Chi-Hungcheng, “*Response Rotor Dynamics of High-Speed Machine Tool Spindle*”, Journals papers on Machine tool applications, 2011
- [3] Momir Šarenac, Mechanical Faculty University of Srpsko Sarajevo, “*Stiffness Of Machine Tool Spindle As A Main Factor For Treatment Accuracy*” *Mechanical Engineering* Vol.1, No 6, 1999 pp. 665 – 674
- [4] A. S. Delgado, E. Ozturk, N. Sims, “*Analysis of Non-Linear Machine Tool Dynamic Behaviour*”, 5th International Conference, Manufacturing Engineering Society– Zaragoza – June 2013.
- [5] Syath Abuthakeer.S, “*Dynamic characteristics analysis of high speed motorized spindle*”, Journal papers on Machine tool applications, 2011.
- [6] Mohanram P.V, “*Dynamic and thermal analysis of high speed motorized spindle*”, Journal papers on Machine tool applications, 2011.
- [7] Jui P. Hung, Yuang L Lai, Tzuo.L. Lio, “*Prediction of the Dynamic Characteristics of a Milling Machine Using the Integrated Model of Machine Frame and Spindle Unit*”, Journal papers on Machine tool applications,2012.
- [8] Jun Wang, Cheog Yao, “*Modeling and Modal Analysis of Tool Holder-Spindle Assembly on CNC Milling Machine Using FEA*”, Journal papers on Machine tool applications, 2012.
- [9] Yuzhong cao,Y, “*Altintas modelling of spindle-bearing and machine tool systems for virtual simulation of milling operations*”, Journal papers on Machine tool applications, 2010.
- [10] Li Da Zhu, “*Modal Analysis and Optimization of Spindle Box of Turn-Milling Centre Based on Finite Element Method*”, *Journal papers on Machine tool applications*, 2010